Title
Compaction-Induced Biochar Loss from Stormwater Biofilters

Author
Le, Huong Truong Diem

Publication Date
2019

Peer reviewed|Thesis/dissertation

UNIVERSITY OF CALIFORNIA

Los Angeles

Compaction-Induced Biochar Loss from Stormwater Biofilters

A thesis submitted in partial satisfaction of the requirements for the degree Master of Science in Civil Engineering

by

Huong Truong Diem Le

2019

ABSTRACT OF THE THESIS

Compaction-Induced Biochar Loss

from Stormwater Biofilters

by

Huong Truong Diem Le

Master of Science in Civil Engineering

University of California, Los Angeles, 2019

Professor Sanjay K. Mohanty, Chair

Roadside biofilters can transform the nation's millions of miles long road infrastructure into an integrated stormwater treatment system. However, unlike traditional biofilters, roadside biofilter media may need to be compacted to maintain required soil stability. Thus, it is critical to examine how amendments used in biofilters behave under compaction. The objective of this work is to examine the effect of the size of biochar, a carbonaceous soil amendment, on the performance of biochar-augmented biofilters subjected to compaction. To examine the effect of biochar particle size on hydraulic properties and contaminant removal capacity of biofilters, a mixture of sand (0.6-0.8 mm) and biochar (5% by weight) with three size ranges (150 μm < d < 833 μm, 833 μm < d < 1180 μm and 1180 μm < d < 2000 μm) was packed in plastic columns (5.1 cm I.D. and 30.5 cm media length) using compaction energy similar to Standard Proctor method, and subjected to intermittent infiltration of stormwater. Results showed that the particle size of biochar did not

significantly affect the quantity of particles released during intermittent infiltration of stormwater, and the quantity of biochar released was insignificant compared to the biochar remained in the biofilter. To examine the dominant mechanism of particle release after compaction, biochar particles of different sizes were coated with a dye (acridine orange), subjected to compaction, and the dye concentration in the released biochar particles was compared against the concentration in packed biochar from where the fine particles were released from. The results showed that disintegration, not abrasion, is the dominant mechanism for biochar release under compaction, and disintegration is particularly prominent when biochar size was small. Biofilters with larger biochar size exhibited the highest initial hydraulic conductivity and the least potential to clogging. However, biofilters with high particle sizes had the lowest *E. coli* removal capacity. Overall, these results indicate that the negative impact on compaction can be mitigated by using the size of biochar similar to or greater than the size of other biofilter's media such as sand.

The thesis of Huong Truong Diem Le is approved.

Jennifer A. Jay

Michael K. Stenstrom

Sanjay K. Mohanty, Committee Chair

University of California, Los Angeles

2019

Table of Contents

List of Figures vi
List of Tables vii
List of Acronyms viii
Acknowledgements ix
1. Introduction 1
2. Materials and Methods 4
2.1. Natural and Synthetic Stormwater 4
2.2. Biofilter media and mixture with different biochar size 4
2.3. Column design and hydraulic characteristics 5
2.4. Release of biochar particle from column during intermittent infiltration of stormwater. 7
2.5. Measurement of hydraulic conductivity 8
2.6. Measurement of effective pore volume and flow path heterogeneity 9
2.7. E. coli removal 10
2.8. Clogging potential biofilters with varying biochar size particles 11
2.9. Biochar breaking mechanism during compaction 11
2.10. Statistical analysis 13
3. Results 14
3.1. Pore volume and diffusion process were affected by biochar particle size 14
3.2. Particle size affected hydraulic conductivity under compaction condition 15
3.3. Clogging time of compacted biofilters varied with biochar size 15
3.4. Quantity of particle released by the biofilter did not depend on biochar's particle size 16
3.5. Removal of E. coli depended on biochar size in biofilters 17
3.6. Breakage mechanism depended on particle size of biochar 18
4. Discussion 21
4.1. Cause of decrease in hydraulic conductivity with biochar size 21
4.2. Release of biochar particles after compaction of biofilters was independent of particle size 22
4.3. Biochar particles release mechanisms 22
4.4. E. coli interaction with different biochar particle size 23
5. Conclusion 25
6. References 27

List of Figures

Figure 1. Samples of three biochar fraction sizes: small (150 μm < d < 833 μm), medium (833 μm < d < 1180 μm) and large (1180 μm < d < 2000 μm). The mean size of the sand particles was 750 μm, which is near the limit (833 μm) separating the fine biochar particles from the medium. 5
Figure 2. Triplicates columns for each biochar size fraction (total 9 columns) were used to quantify the effect of biochar particle size on their performance in biofilters subjected to compaction. 6
Figure 3. (A) Breakthrough curves of bromide (tracer) in columns filled with compacted biochar of three sizes: small biochar (SB), medium biochar (MB), and large biochar (LB). (B) Effect of biochar size on pore volume calculated based on volume of stormwater required to achieve relative breakthrough concentration of 0.5. (C) Change in concentration of bromide during flow interruption. Triplicated columns were used for each biochar size. 14
Figure 4. Hydraulic conductivity of columns packed with biochar (5% by weight) of different size ranges. Measurements were conducted in triplicated columns and repeated 6 times per column (n = 18). 15
Figure 5. (A) Effect of suspended solids loading on the hydraulic conductivity (Ks) of biofilters compacted with sand-biochar mixture. (B) Relative reduction of hydraulic conductivity $(KsKs0)$ for each biofilter type; $\Delta Ks\Delta SS$ indicates the slope of each linear model. Hydraulic conductivity was measured during each injection of suspended solids using the Falling-Head method. 16
Figure 6. Release of particles from compacted biochar-sand biofilters during intermittent infiltration of stormwater. Points represent average concentration of triplicated columns of each biochar type and the shaded area represents one standard deviation over mean. The vertical dashed lines indicate the start of a rainfall event after 24 hours of intermediate drying period. 17
Figure 7. Removal of E. coli during rainfall events. The error bars indicate one standard deviation over mean from triplicate columns with duplicate measurements per column (n = 6). The vertical dashed lines indicate the start of a rainfall event. 18
Figure 8. Biochar concentration (circle) and fluorescence intensity (diamond) of biochar particles released from column packed using a Standard Protector method with a mixture of sand and small biochar particles (a) and large biochar particles (b). 19
Figure 9. Variation of fluorescence intensity of biochar particles from standards (grey) and samples (colored) with respect to their concentration as measured by absorbance (m^{-1}). 20
Figure 10. Dye intensity of biochar particles normalized to the biochar concentration was compared for both biochar packed (grey) in the columns and the biochar particles released from the packed column (colored). 20

List of Tables

Table 1. Pore volume and physical characteristics of sand mixed with different biochar size fractions. Mean and standard deviation over mean for each column was estimated from measurements in triplicate columns. 7

List of Acronyms

SB	Mixture of small biochar size
MB	Mixture of medium biochar size
LB	Mixture of large biochar size
BI	Breakage index
FI	Fluorescence intensity
ABS	Absorbance
HPDE	High density polyethylene plastic
I.D.	Inner diameter

Acknowledgements

I would like to express my sincere gratitude to my advisor Dr. Sanjay K. Mohanty for his extraordinary support of my academic journey, for his enthusiasm, thoughtfulness and tremendous knowledge. I would also thank for his invaluable guidance, suggestions and comments in helping me in completing this thesis research. I would like to thank Dr. Jennifer A. Jay for allowing me to utilize the instrument in her laboratory. I thank the committee —Dr. Michael K. Stenstrom, Dr. Jennifer A. Jay, and Dr. Sanjay K. Mohanty— for their assistance in revision of the thesis.

I would like to thank my fellow lab mates in the Mohanty research group for their wonderful collaboration, including Renan Valenca, Annesh Borthakur, and Maryam Ghavanloughajar. I am thankful to Renan, for his assistance in critical analysis of data; to Annesh, for his contribution in developing the method; to Maryam, for her instruction on how to use different lab instruments in spite of her busy schedule.

A very special vote of thanks to the California Department of Transportation for helping the funding of the research work. I also thank Biochar Supreme LLC for providing the qualified biochar for this work. And finally, I am grateful to all of my colleagues at the Department of Civil and Environmental Engineering at UCLA for their incredible kindness and professionalism. I truly feel being with my family throughout the time of my M.S. study. UCLA and all of you will always be a part of my heart in my long journey ahead.

Sincerely,

Huong Truong Diem Le

1. Introduction

Roadways and other transport-related surfaces account for 15-20% of the urban surface and can constitute up to 70% of total impervious area (Rodrigue et al., 2017; Wong et al., 2000). The impervious surfaces that replace the natural landscape not only increase runoff volume (Cambi et al., 2015) but also increase contamination of surface waters (Yang and Toor, 2018; Walsh et al., 2012). During a typical rainfall, stormwater runoff washes off pollutants accumulated on roadways during dry weather and contaminates the waterbodies. To decrease the negative impacts of roadways on stormwater quantity and quality, roadside biofilters can be designed, which can provide other additional benefits including groundwater recharge, carbon sequestration and ecological habitat restoration (Wong et al., 2000).

One major obstacle in implementing roadside biofilters is that the soil needs to be compacted, and compaction typically decreases the infiltration capacity of the soil (Currie 1984; Ares et al., 2005; Frey et al., 2009; Berli et al., 2004). Compaction changes increases the bulk density of the soil and decreases soil porosity (Gupta et al., 1989; Boone, 1988), which in turns could lower infiltration of water in biofilters (Pitt et al., 2008; Mossadeghi-Bjorklund et al., 2016). The effect of compaction on soil depends on the soil texture. For instance, low colloid-content media such as silt loam is more likely to be affected by soil compaction than medium or finely textured media such as loamy and clayey soils, whereas sandy soil is the least susceptible to soil compaction (Horn et al., 1995). While addition of sand as bulking agent can increase infiltration capacity of biofilters, it can also decrease contaminant removal. Thus, other amendments with higher contaminant removal capacity can be used to compensate for a decrease in removal after the addition of sand. Among different types of amendments, biochar has been increasingly used in stormwater biofilters to enhance the contaminant removal capacity of the biofilters (Mohanty et al., 2018). However, its performance has never been tested under compaction. In particular, it is not clear how compaction may affect biochar

properties and its ability to infiltrate and treat stormwater. Improving the knowledge of how compaction may alter biochar performance in biofilters can help develop design strategies to alleviation the impact of compaction on biochar in biofilters.

The degree of the fracture depends on particle strength (Tavares and King, 1998). As biochar's load bearing capacity is lower than other soil amendment materials such as woodchip, compost and sand (Reza et al., 2012), it is likely that biochar may break under compaction and release child fragments and fine particles. The breaking mechanism can have contrasting effect on contaminant removal or release in biofilters. For example, fragmentation of biochar particles can increase surface area and provide new surface for adsorption of pollutants. On the other hand, if the energy of compaction is lower than the tensile strength of biochar, biochar may slide through the pores or rearrange in pore spaces to absorb the compaction energy, and in this process, the surface of particles can be peeled off by abrasion (Chan et al., 1983). This would result in the release of surface coating that may have accumulated pollutants. Thus, it is important to determine the dominant breakage mechanism for biochar under compaction.

Compaction could also release fine biochar particles and clog the pores, which could ultimately decrease the hydraulic conductivity of biochar-augmented biofilters, like any other amendments. However, the extent to which it can decrease hydraulic conductivity has not been evaluated. In particular, it is not clear how the relative size of biochar with respect to the bulking agent such as sand can affect the its behavior under compaction. The size distribution and quantity of fragments generated after compaction can depend on the breakage mechanism, which is constrained by the particular shape and size of initial soil particles (Tavares and King, 1998; Zhang and Baudet, 2013). Thus, it is critical to understand if biochar size can be used as a design factor to maximize its performance in roadside biofilters under compaction.

The objective of this study was to investigate the effect of biochar size on their performance —hydraulic or infiltration capacity and contaminant removal— in biochar-

augmented biofilters subjected to compaction. The underlying hypotheses of this study were biochar size will influence biochar breakage mechanisms during compaction, hydraulic conductivity or clogging potential, and the contaminant removal capacity of biochar-augmented biofilters after compaction. The results provide insights on how biochar behaves under compaction in roadside biofilters during their construction.

2. Materials and Methods

2.1. Natural and Synthetic Stormwater

Natural stormwater was used to examine the bacterial removal capacity of compacted biochar, whereas synthetic stormwater with electrical conductivity and pH similar to natural stormwater without particles was used to examine biochar leaching after compaction. Natural stormwater was collected using 20-L HPDE plastic carboys from the Ballona Creek in Los Angeles, CA (34° 0'36'' N, 118° 23'29'' W), which receives dry-weather irrigation runoff from 318 km^2 urban area with 82% developed and 61% impervious surface (Gold et al., 2015). The stormwater was characterized for pH, conductivity, and turbidity within 1 hour of sample collection, and stored in a refrigerator at 4ºC to minimize the bacteria growth. Before use in the experiment, large particulates were removed by gravimetric settling, and stormwater temperature was raised to room temperature. Synthetic stormwater was prepared by adding 10mM NaCl to deionized (DI) water and adjusting the pH to 7.8 ± 0.2 using HCl. Use of synthetic stormwater without particulates at consistent pH and ionic strength - the chemical driver for particle release or deposition - helps quantify the effect particle size on the potential of biochar release after compaction.

2.2. Biofilter media and mixture with different biochar size

Commercially available biochar (Biochar Supreme, Everson, WA) and sand (20-30 Ottawa Sand, Certified) were selected for this study. The sand was washed with DI water. Washed sand and biochar were oven-dried at 100 °C overnight. To understand the effect of the diameter (d) of biochar particles on their physical integration during and after compaction, biochar was sieved to remove particles smaller than 150 μm (sieve# 100) and greater than 2000 μm (sieve# 10). Pre-removal of fine particles ensured that any particles released during the

experiment were produced by compaction during the packing of biochar in columns, whereas removal of gravel-sized biochar minimized preferential flow path in the packed columns.

To examine the effect of particle size, three fractions of biochar were created by sieving: small (150 μm < d < 833 μm), medium (833 μm < d < 1180 μm) and large (1180 μm < d < 2000 μm) (Figure 1). Biochar (5% by weight) was mixed with sand in a glass container to create a homogeneous mixture before using the mixture to pack the columns.

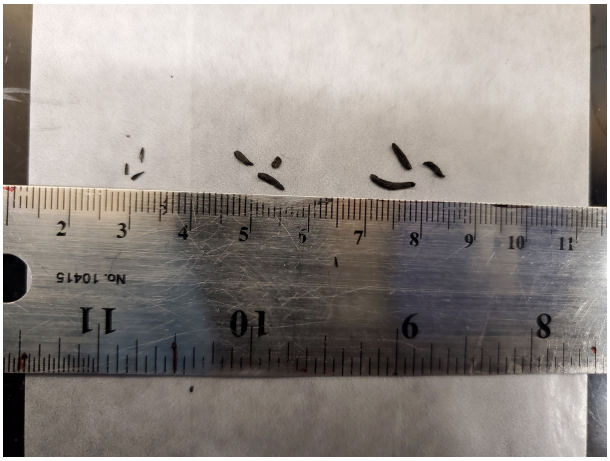

Figure 1. Samples of three biochar fraction sizes: small (150 μm < d < 833 μm), medium (833 μm < d < 1180 μm) and large (1180 μm < d < 2000 μm). The mean size of the sand particles was 750 μm, which is near the limit (833 μm) separating the fine biochar particles from the medium.

2.3. Column design and hydraulic characteristics

To design the laboratory column setup, PVC pipes (5.1 cm I.D. and 30.5 cm length) and fitting were used. The pipes were glued with PVC fittings and connected to a control valve to regulate the effluent flow. Triplicate columns were prepared for each media mixture (Figure 2). A nylon screen (100 μm opening size) was inserted at the bottom of the column to prevent the larger biochar particles from washing off the biofilters. A 9-cm layer of gravel was poured over the screen to create a drainage layer, and a second nylon screen (# 75 μm mesh) was placed on top of the gravel layer to prevent the sand-biochar mixture from falling into the pore space between the gravels.

Figure 2. Triplicates columns for each biochar size fraction (total 9 columns) were used to quantify the effect of biochar particle size on their performance in biofilters subjected to compaction.

The sand-biochar mixture was added incrementally and compacted to a height of a 3.8-cm layer using a Proctor hammer (2.5 kg). In order to maintain the equivalent energy of a standard Proctor test that would be applied on the filter media, the hammer was dropped 7 times from 30.5 cm height per layer (Equation 1) .

$$\text{Number of blow per layer} = \frac{\text{E} \times \text{V}}{\text{W} \times \text{N} \times \text{H}} \quad (1)$$

where energy per unit volume (E), hammer weight (W), number of total layers (N) and drop height (H) were kept constant as 593 kN-m m^{-3}, 2.5 kg, 3 layers and 30.5 cm (Das, 2009). The single layer height of filter media was calculated by dividing the column area by the column volume and it equaled 3.8 cm or 0.001 m^3 for volume. The procedure was repeated until the filter media depth reached 30.5 cm with a total of 8 layers.

The bulk density was measured for each layer to confirm the uniform distribution of filter media by depth. A 2.5-cm layer of gravel was placed on the top of the filter media to prevent an

erosion biochar during stormwater infiltration or floating of biochar particles during ponding of the filter layer. To remove the air from voids between sand and biochar particles, DI water was applied through the bottom outlets in an upward direction using gravity until the filter media layer was completely saturated. The pore volume of different layers was measured by subtracting the dry weight from the saturated weight. For instance, the pore volume of the bottom drainage layer was calculated by measuring the volume of water required to fill the drainage (75.4 ± 11.3 mL). The pore volume of the filter layer (sand-biochar media) was calculated by subtracting the pore volume of the bottom drainage layer from the pore volume of the entire media column until the bottom of the top gravel layer. The porosity of the column was estimated by diving the measured pore volume by the empty bed volume. Packing parameters were summarized in

Table 1.

Table 1. Pore volume and physical characteristics of sand mixed with different biochar size fractions. Mean and standard deviation over mean for each column was estimated from measurements in triplicate columns.

Biochar type	**Biochar size range (μm)**	**Bulk density (g cm^{-3})**	**Pore volume of filter layer (mL)**	**Pore volume including drainage layer (mL)**	**Porosity (%)**
Small	150 - 833	1287.8 ± 21.7	210.3 ± 13.2	302.7 ± 5.3	26.4 ± 1.7
Medium	833 - 1180	1245.5 ± 31.1	329.9 ± 65.0	409.1 ± 61.8	41.4 ± 8.1
Large	1180 - 2000	1242.3 ± 13.8	404.4 ± 16.2	484.0 ± 15.0	50.7 ± 2.0

2.4. Release of biochar particle from column during intermittent infiltration of stormwater.

To examine the release of biochar particles from the biofilters during rainfall events, synthetic stormwater without particles and adjusted to pH and ionic strength of actual stormwater was used in order to provide a consistent condition to compare particle leaching by physical factors. Synthetic stormwater was applied on the top of filter media at a flow rate of 8.5 mL m^{-1} or flux of 25.2 cm h^{-1}, and effluent samples were collected at the bottom of the biofilters with an interval of 14 minutes (~100mL) into 250-mL amber bottles. The pump was stopped after 48 min, and the bottom valve of the column was closed to prevent water drainage. The volume of the sample was measured by recording weight, and the turbidity, an indicator of biochar concentration, was estimated by measuring absorbance at 890 nm using a UV-Visible spectrophotometer (Perkin PerkinElmer, Lambda). The concentration of particles (mg L^{-1}) was estimated from the absorbance of samples by using a calibration curve of the absorbance of samples containing a known concentration of biochar particles. The total biochar particles released during a rainfall event from a column was estimated by summing the multiplication of concentration to the volume in each fraction. The experiment was repeated every day for 5 continuous days to examine if the quantify of particle release varies with successive rainfall events.

2.5. Measurement of hydraulic conductivity

The saturated hydraulic conductivity (K_s, mm h^{-1}) of each column was measured using Falling Head method (Equation 2):

$$K_s = \frac{L}{t} \ln\left(\frac{h_1}{h_2}\right) \quad (2)$$

where L is the depth of filter media layer (mm), h_1 is the initial height of water column above the filter media measured from the outlet at the bottom (mm), h_2 is the final height of water column

about the filter media after draining of water for a duration t. Before the measurement, the column was first saturated by injecting synthetic stormwater in an upward direction until the water level reached ~10 cm above the top gravel layer. This initial height of water (h_1) was marked, and a second mark (h_2) was made 5 cm below the first mark. Effective hydraulic conductivity of each column was determined by measuring the volume released and the time required to drain the water from h_1 to h_2 by opening the bottom valve of the column. The difference in the head ($h_1 – h_2$) was verified by dividing the volume of water drained with the surface area of the water column. The experiment was repeated 6 times in each column (total of 18 measurements per biochar size fractions).

2.6. Measurement of effective pore volume and flow path heterogeneity

During a rainfall event or application of stormwater from the top, the entire pore spaces are not filled with stormwater due to the presence of air in the void space. Thus, the effective or operational pore volume, the fraction of total pore space being saturated during an infiltration event, would be smaller than the saturated pore volume measured by gravimetry. To measure the effective pore volume of the filter media, a tracer test was performed on each column using bromide as a conservative tracer. Synthetic stormwater containing bromide (9mM NaCl + 1mM KBr) was used during the tracer study. Synthetic stormwater (10 mM NaCl) without bromide was applied for an hour to flow equilibrium during a short rainfall event before the injection of bromide solution. Approximately 600 mL stormwater containing bromide was applied from the top of each column at 8.5 mL min^{-1} for 70 min before switching the solution to the stormwater without bromide for an additional 50 min to flush bromide solution from the pore water. The valve at the bottom was closed after the experiment to prevent drainage, and the flow was interrupted to examine if the residual bromide concentration in pore water would change during flow interruption. The flow was resumed after 12 h by applying 300 mL of bromide-free stormwater for 30 min. This period is enough to permit bromide ions to diffuse from the pore

water inside the biochar to bulk pore water against the concentration gradient, thereby increasing the bromide concentration in pore water (Brusseau et al., 1997). The ratio of bromide concentration before and after the flow interruption is used as the indicator for the presence of diffusion-limited zones in compacted biochar of different size fractions. During the injection of stormwater, 43 – 85 mL of effluent samples were collected at 5 – 10 min intervals and 10 mL of the sample fraction was centrifuged to remove any particulates before the measurement of bromide concentration using an Ion Chromatography (Dionex™ Integrion™ HPIC™ System, ThermoFisher). Effective pore volume was measured by estimating the volume of stormwater injected to increase the effluent bromide concentration to 50% of the feed solution containing 1 mM bromide.

2.7. E. *coli* removal

To examine the removal of bacteria in biofilters, a kanamycin-resistant *Escherichia coli* (*E. coli*) strain (NCM 4236) was used to distinguish the applied *E. coli* from other strains present naturally in stormwater. *E. coli* were suspended in stormwater following a method outlined elsewhere (Mohanty et al., 2014). Briefly, *E. coli* were cultured to a stationary phase, centrifuged and washed with phosphate buffer solution to remove the growth medium, and suspended in the collected stormwater to achieve an initial concentration of nearly 10^6 colony forming units (CFU) mL^{-1}.

Approximately 5 pore volumes of contaminated stormwater were injected into each column at a flow rate of 8.5 mL m^{-1}. Effluent waste was collected at the bottom using a 1-L beaker to estimate the volume that had passed through the system. Based on prior study (Mohanty et al., 2014), *E. coli* breakthrough is expected to occur after the injection of 2 pore volume of stormwater. We collected that last 10 mL of sample to determine the removal (worst case scenario). 50 uL of the sample was spread evenly over the surface of the agar plate containing kanamycin, and the plates were incubated in the oven at 37°C for 18-24 hours.

Effluent concentration (CFU/mL) of each column was estimated by multiplying the visible colony forming unit (CFU) on each plate with the appropriate dilution factor. Each sample was enumerated on duplicate agar plates at one decimal dilution. Concentrations calculated using plates with between 30 and 300 CFU were averaged to obtain *E. coli* concentration. The log-removal of *E. coli* from stormwater during the attachment phase was calculated using the equation: log removal or removal capacity = $-\log(C/C_0)$, where *C* is the steady-state effluent concentration and C_0 is the influent concentration. The experiment was repeated for 5 consecutive days to examine any change in bacterial removal.

2.8. Clogging potential biofilters with varying biochar size particles

In the end, the clogging potential of each biochar fraction was measured by injecting stormwater containing a high concentration of sediments. Turbid water was prepared by mixing tap water with soil collected from the Ballona Wetland in Los Angeles. The wetland receives dry- and wet-weather stormwater runoff throughout the year. The soil was dried and sieved to select the particle size smaller than 90 μm (U.S Standard # 170) and mixed in water to achieve as total solid of 3.0 g L^{-1}, which was similar to the maximum TSS (2.0 – 4.0 g L^{-1}) found in urban stormwater runoff (Lin, 2004). Turbid water was poured on top of each column to create a ponded layer, and the hydraulic conductivity was monitored using the Falling Head method described earlier.

2.9. Biochar breaking mechanism during compaction

To examine how biochar may break during compaction, small and large biochar were coated with Acridine Orange dye (Fisher Scientific, Waltham, MA), and the concentration of dye in the broken biochar fragments released during infiltration study was compared with the dye concentration in the packed biochar. 25g of biochar of each size were mixed at 450 rpm with 500 mL of dye (Acridine Orange, 10 g/L) in a 1-L glass beaker using a stirrer and a spin bar.

The glass beaker was covered with aluminum foil to minimize dye decay due to light exposure. After 30 min, particles were washed under running tap water to remove excess dye. The washed particles were spread as a thin layer over the surface of 5 sieve containers (U.S Standard # 200) and placed in the oven at 50°C for 3 hours. After drying, biochar was sieved again using the appropriate sieve numbers for each size range (small fraction size 150 μm < d < 833 μm and large fraction size 1180 μm < d < 2000 μm) to remove any fine particles generated during sample preparation. The dyed biochar was mixed with sand and packed in columns using the method described earlier (section 2.3) up to a filter media height of 11.4 cm.

In order to release biochar particles that may have been created during compaction, synthetic stormwater was poured on the top of the filter media to create a ponding layer, and the effluents were collected at regular intervals. The average concentration of dye in biochar was measured by grinding 2 g of dyed biochar, and the dye intensity of suspension containing ground biochar at different concentrations was measured to determine the standard calibration curve. To minimize the interference of dissolved dye, all samples and calibration standards were centrifuged at 4000 rpm for 15 minutes at room temperature. The supernatant fluid was removed, and the settled biochar was vortexed in 2 mL of DI water before analyzing for absorbance at 890 nm (UV spectrophotometer, PerkinElmer), which is a measure of turbidity or biochar concentration, and fluorescence intensity for excitation and emission at 460 and 650 nm (GloMax Discover, Promega), which is a measure of dye concentration on the biochar.

A Breakage Index (BI) was developed to quantify the breakage mechanism, which relates dye intensity (FI) to the absorbance of biochar particle (ABS) (Equation 3).

$$BI = \frac{FI\ (intensity)}{ABS\ (absorbance)} \quad (3)$$

It was assumed that the dye concentration in the fragments will be higher than the mean value in biochar before compaction if the fragments are released from the surface of particle by abrasion, and the dye concentration will be lower if the fragments are released as a result of

intra-particle fragmentation of biochar. Thus, if BI from effluent samples were higher than BI from the standards (bulk biochar in the column), the breakage mechanism is due to abrasion. Conversely, if BI from column samples is lower than BI from standards, the breakage mechanism is due to fragmentation.

2.10. Statistical analysis

One-way analysis of variance, ANOVA, was performed using R (version 3.6.1) between data sets to compare the parameters measured or estimated as a function of biochar particle size. The significance of differences between two specific means was assessed with the Tukey HSD post-hoc comparison test. Differences were considered significant at a *p*-value of less than 0.05.

3. Results

3.1. Pore volume and diffusion process were affected by biochar particle size

Biochar size in compacted biofilters affected the biofilter's pore volume and matrix diffusion in the filter layer, but this effect was more apparent in columns with small biochar particles (Figure 3). he effective pore volume of the compacted biochar biofilters decreased with increases in particle sizes. The pore volume of columns with small biochar was 19% higher than columns with medium biochar and 23% higher than the columns with large biochar. Compaction is expected to increase the tortuosity of the flow path and potentially increase moisture content trapped in pores, which could increase matrix diffusion. Concentration changes during flow interruption, a measure of matrix diffusion, was highest in columns with large biochar. A decrease in particle size did not consistently change the extent of matrix diffusion in compacted biochar columns.

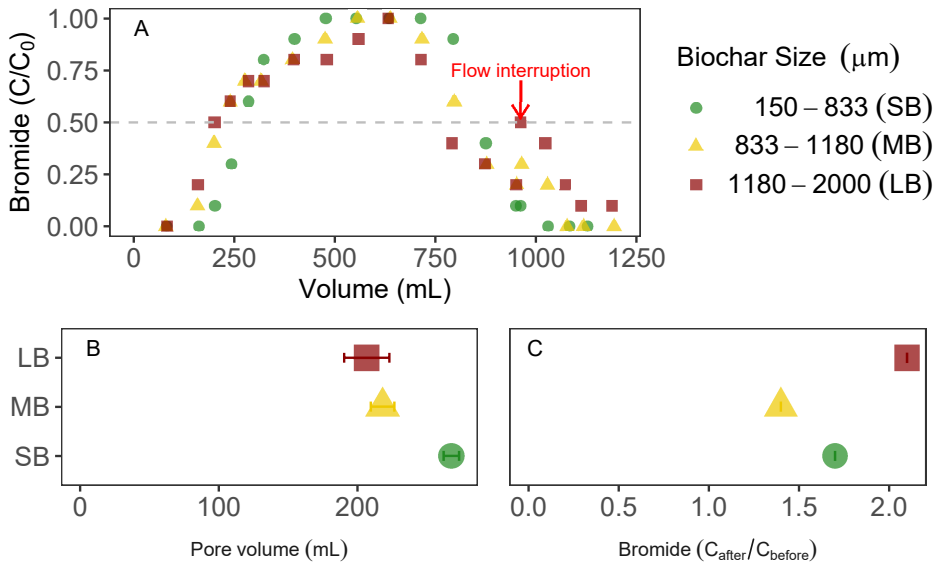

Figure 3. (A) Breakthrough curves of bromide (tracer) in columns filled with compacted biochar of three sizes: small biochar (SB), medium biochar (MB), and large biochar (LB). (B) Effect of biochar size on pore volume calculated based on volume of stormwater required to achieve relative breakthrough concentration of 0.5. (C) Change in concentration of bromide during flow interruption. Triplicated columns were used for each biochar size.

3.2. Particle size affected hydraulic conductivity under compaction condition

Hydraulic conductivity of compacted biochar-sand columns decreased with reduction in biochar size (Figure 4). While the hydraulic conductivity of columns with large biochar was 2579 ± 218 mm h^{-1}, the hydraulic conductivity did not significantly change (2477 ± 216 mm h^{-1}) for medium biochar. However, reducing the biochar size to small range significantly decreased ($p < 0.05$) the hydraulic conductivity to 1520 ± 119 mm h^{-1}, which is nearly 40% lower than the columns with medium or large biochar.

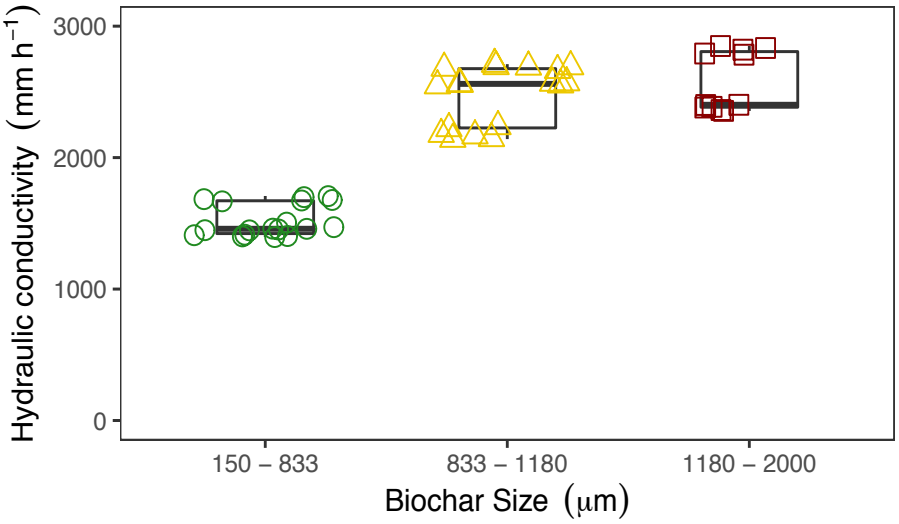

Figure 4. Hydraulic conductivity of columns packed with biochar (5% by weight) of different size ranges. Measurements were conducted in triplicated columns and repeated 6 times per column (n = 18).

3.3. Clogging time of compacted biofilters varied with biochar size

The hydraulic conductivity of the biofilter decreased with the injection of stormwater containing a very high concentration (3 g/L) of sediment (Figure 5). The rate at which hydraulic conductivity decreased with increases in solid loading is used as an indicator of the biofilters' clogging potential. The clogging potential decreased with increases in the size of biochar particles in biofilters (Figure 5 – B).

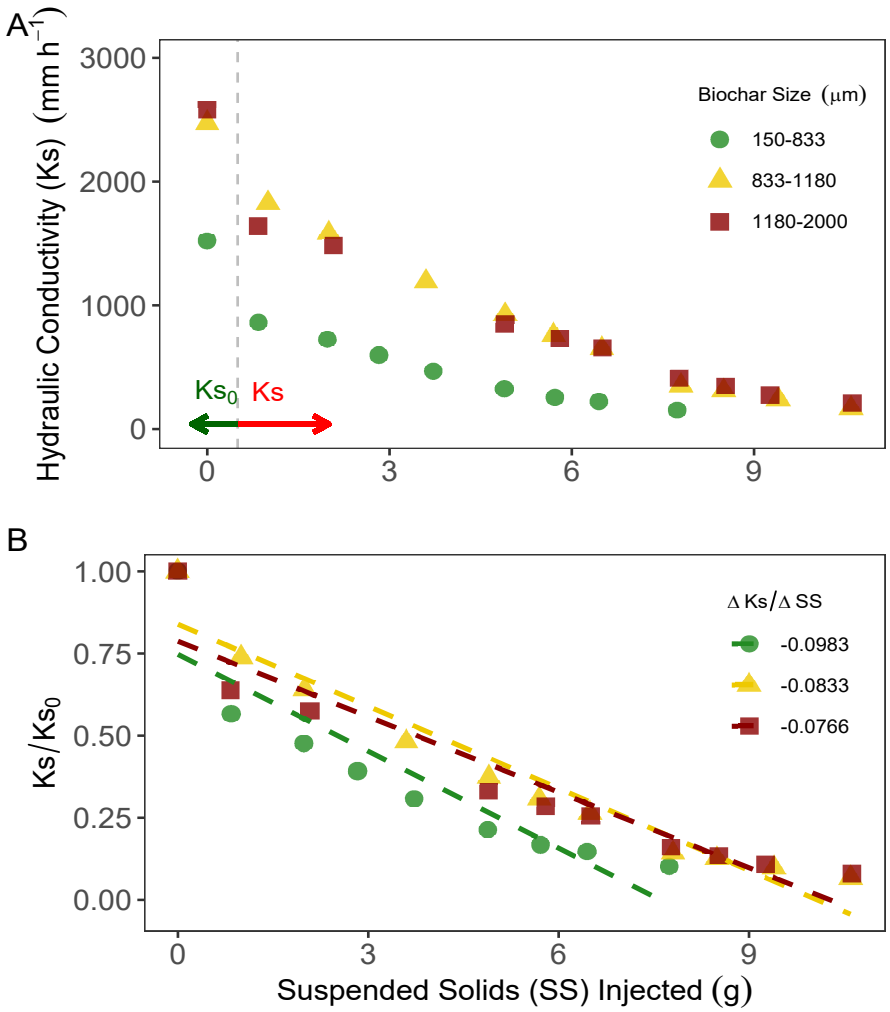

Figure 5. (A) Effect of suspended solids loading on the hydraulic conductivity (Ks) of biofilters compacted with sand-biochar mixture. (B) Relative reduction of hydraulic conductivity (Ks/Ks_0) for each biofilter type; $\Delta Ks/\Delta SS$ indicates the slope of each linear model. Hydraulic conductivity was measured during each injection of suspended solids using the Falling-Head method.

3.4. Quantity of particle released by the biofilter did not depend on biochar's particle size

Compacted sand-biochar biofilters released particles during the infiltration of stormwater, but the extent of particle release appeared to be independent of biochar size (Figure 6*Figure 6*). During a rainfall, the concentration of biochar in the effluent peaked initially and decreased as more stormwater passed through the biofilters. The peak concentration decreased in successive rainfall events, although after 3 rainfall events, the peaks did not decrease any further indicating

exhaustion of the pool of biochar particles available for release. Similarly, the cumulative mass of biochar particles released from the biofilter appears to be independent of biochar particle size in the biofilters.

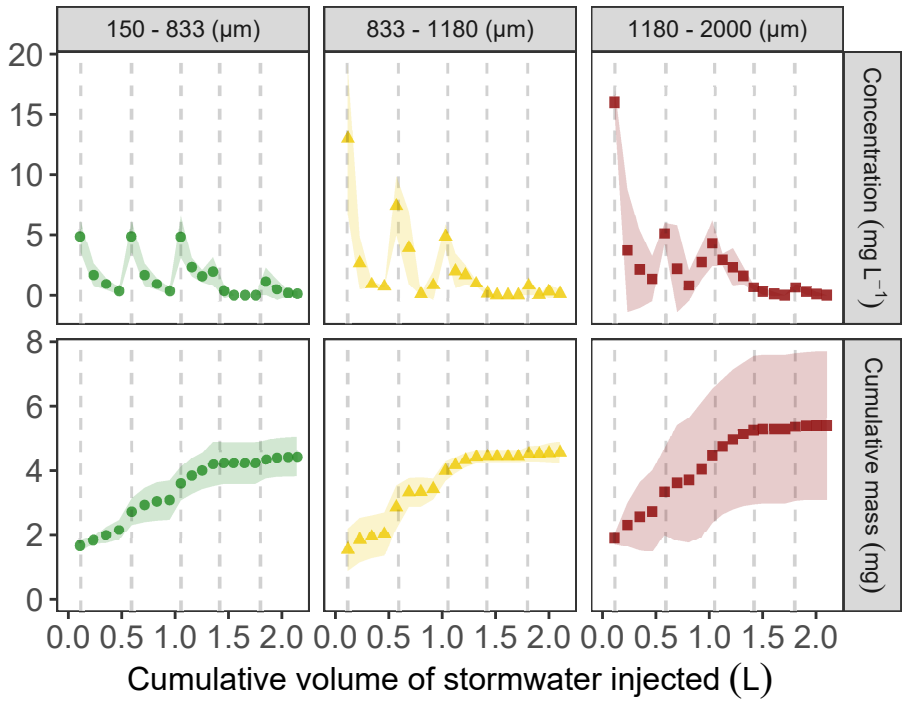

Figure 6. Release of particles from compacted biochar-sand biofilters during intermittent infiltration of stormwater. Points represent average concentration of triplicated columns of each biochar type and the shaded area represents one standard deviation over mean. The vertical dashed lines indicate the start of a rainfall event after 24 hours of intermediate drying period.

3.5. Removal of *E. coli* depended on biochar size in biofilters

Biochar size affected the removal of *E. coli* (Figure 7). Although consecutive rainfall events significantly decreased the removal capacity of columns with medium and large biochar, the removal capacity of columns with small biochar mostly remained high: the effluent concentration was near detection limit.

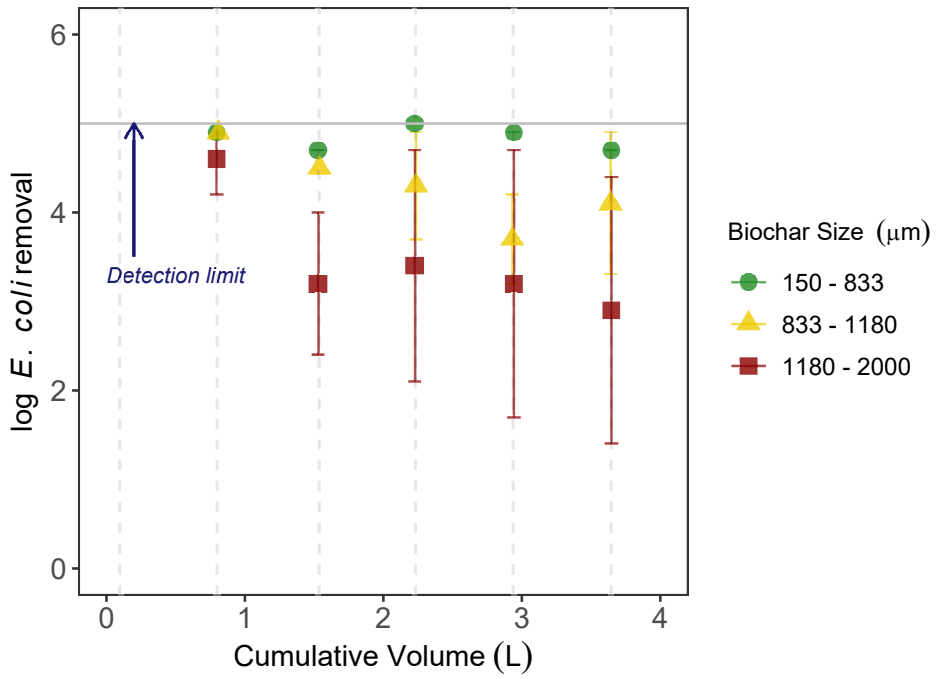

Figure 7. Removal of *E. coli* during rainfall events. The error bars indicate one standard deviation over mean from triplicate columns with duplicate measurements per column (n = 6). The vertical dashed lines indicate the start of a rainfall event.

3.6. Breakage mechanism depended on particle size of biochar

Biochar particles can be broken into smaller pieces under compaction, but how and where they would break depends on the relative size of biochar with respect to the sand. The fluorescence intensity (FI) of biochar mobilized from dye-coated biochar after compaction depended on the size of biochar: while the dye intensity of biochar particles released from the columns with large biochar did not change throughout the experiment, the dye intensity of biochar particles released from the column with small biochar decreased (Figure 8).

The result showed that increase in absorbance increased the FI of both biochar particles compacted in the columns and the biochar particles released from the packed columns. However, the fluorescence intensity of mobile particles released from smaller biochar columns was low compared the biochar particles in the columns. In large biochar columns, the FI of mobile biochar particles and the biochar in columns were similar (Figure 9). For columns with

smaller biochar, the biochar released appears to have lower dye concentration, as indicated by fluorescent intensity, than the biochar in the columns (Figure 10). The difference of dye concentration between packed and released biochar particles was not significant in columns with large biochar. Thus, biochar size appears to control how biochar would break under compaction.

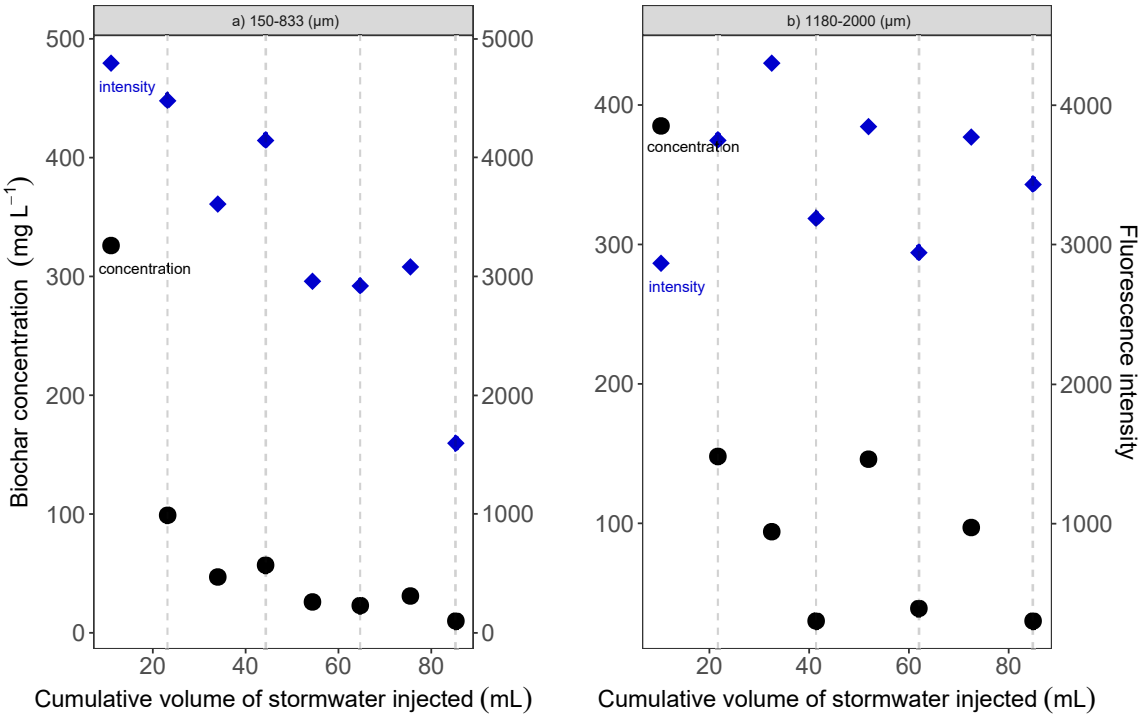

Figure 8. Biochar concentration (circle) and fluorescence intensity (diamond) of biochar particles released from column packed using a Standard Protector method with a mixture of sand and small biochar particles (a) and large biochar particles (b).

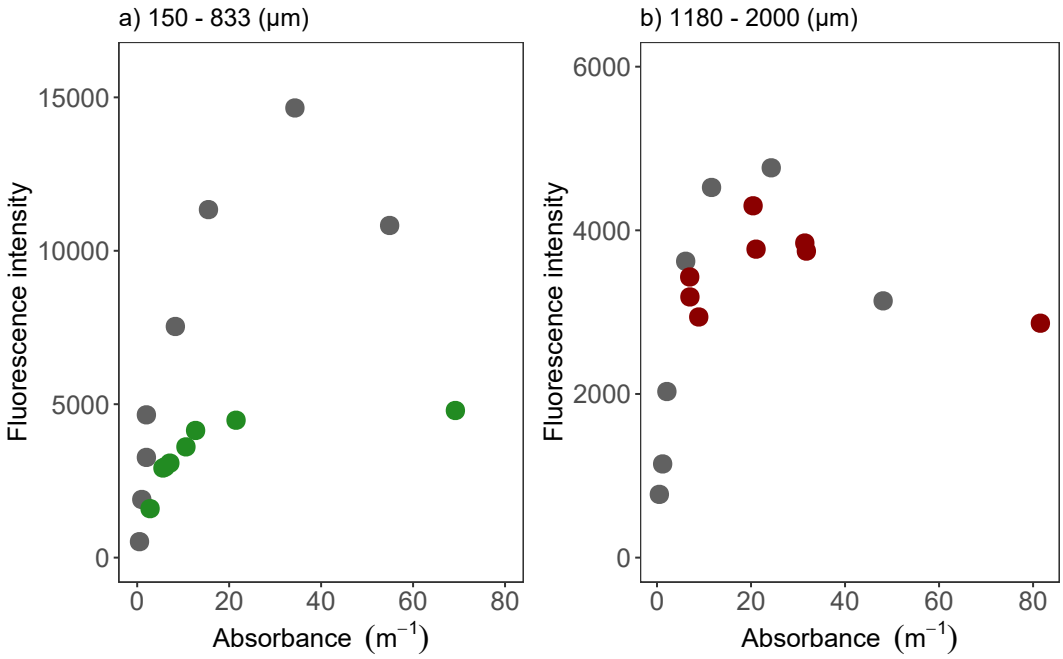

Figure 9. Variation of fluorescence intensity of biochar particles from standards (grey) and samples (colored) with respect to their concentration as measured by absorbance (m^{-1}).

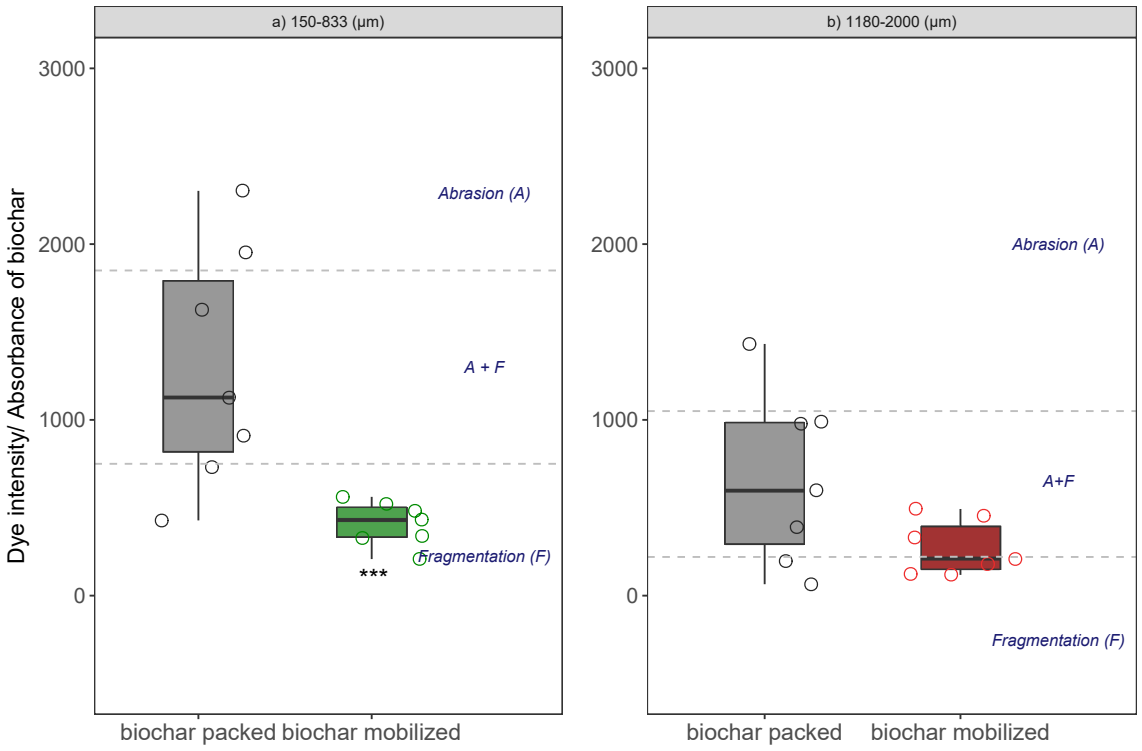

Figure 10. Dye intensity of biochar particles normalized to the biochar concentration was compared for both biochar packed (grey) in the columns and the biochar particles released from the packed column (colored).

4. Discussion

4.1. Cause of decrease in hydraulic conductivity with biochar size

Hydraulic conductivity of biofilters is a measure of the infiltration capacity of biofilters. Thus, it is critical to measure if hydraulic conductivity would change with different design factors and conditions at the sites. Results showed that adding biochar particles smaller than sand particles decreased the hydraulic conductivity of the mixture, whereas adding biochar with size larger than sand did not change the hydraulic conductivity significantly. Smaller biochar particles can slide into the interparticle pores between sand grains, thereby effectively decrease the porosity, and consequently the hydraulic conductivity. On the other hand, the size of large biochar is greater than the pore space between sand grains. Therefore, sand will occupy the space between biochar particles. Thus, the hydraulic conductivity of sand and large biochar mixture would be similar to that of sand and biochar of similar size. The results support previous finding, where the decrease in hydraulic conductivity following the addition of fine biochar particles was the result of increased tortuosity and reduced interpore in the mixture (Liu et al., 2016). Nevertheless, Liu et. al (2016) did not measure hydraulic conductivity of mixture under compaction. Because all mixtures were subjected to same degree of compaction, we show that biochar size has similar effect on hydraulic conductivity of compacted biochar as it does for uncompacted biochar.

The clogging potential of biochar was lower when the biochar size was larger. The decrease in hydraulic conductivity with increase in sediment loading was more severe for smaller biochar than that of large biochar. It was expected that compaction would increase clogging in biofilters. The result in this study confirmed that the extent to which compacted biochar may clog depending on the particle size of biochar, and the larger biochar clogs at a slower rate. Thus, adding biochar larger than sand size (1180 μm < d < 2000 μm) in biofilters

would alleviate the impact of compaction on decrease in hydraulic conductivity of filter media and their clogging rate.

4.2. Release of biochar particles after compaction of biofilters was independent of particle size

Compaction is expected to break biochar particles, which could increase their release or physical loss from biofilters. However, the results showed that the amount of biochar particles released after compaction was insignificant compared to the amount of biochar remained in the biofilters. Therefore, compaction would not increase the physical loss of biochar particles from the biofilters. The quantity of biochar particles released initially after compaction was independent of particle size of biochar. A similar amount of fine biochar discharged from all biofilters indicates that biochar release is independent with initial particle size.

4.3. Mechanism of biochar breakage during compaction

The relative concentrations of dye coating (per unit biomass concentration) in released biochar were different based on biochar size. The relative dye intensity of released biochar was less than the average intensity in smaller biochar size before compaction, which indicates that the dye concentration decreased in discharged biochar with respect to the packed biochar from which they were released from. This occurs if biochar was released by fragmentation of interior sites where dye may not have penetrated. On the other hand, dye concentration in the released biochar was similar to the biochar in columns when biochar size was large, suggesting that fragmentation is not the dominant mechanism for large biochar. The result is in contrast to the initial hypothesis that large biochar would be more susceptible to fragmentation by breaking of biochar interior and release of uncoated biochar particles. We speculate that this could be because of lesser number of biochar particles impacted during compaction. At 5% by weight, small biochar size would have larger number of particles than that large biochar size in the

biofilters. Thus, a greater quantity of smaller biochar particles would be susceptible to breakage than large biochar particles. Assuming fragmentation rates are proportional to the number of biochar available in the biofilter, biofilter containing small biochar would release more particles by fragmentation, which consequently would decrease relative dye concentration.

The result showed that the dye intensity of released biochar was never higher than that of the biochar released from, irrespective of the biochar size. This study proved that a release of coating by abrasion—which occurs when biochar particles rub against each other during compaction—is not the dominant mechanism for particle release during compaction. This is expected because the energy of compaction was much higher than the tensile strength of the biochar (Das et al., 2018). Thus, biochar particles are more likely to break at the interior position than being abraded at the surface under compaction. The lesser likelihood of “peeling” action compared with “fracturing” action during compaction suggests that compaction would break and open the biochar particle, exposing new surface sites for contaminant adsorption. As the result, the release of surface coating, which may have accumulated high concentration of contaminant, is less of a concern.

4.4. *E. coli* interaction with different biochar particle size

Our results showed that log *E. coli* removal was higher in columns containing smaller biochar. This is expected because smaller biochar (for same weight percentage) should have greater number of biochar particles with high surface area compared with the larger biochar. The result with different particle size is similar to the outcome reported previously Mohanty and Boehm (2014), where *E. coli* removal capacity reduced from 96% to 62% in biochar-sand columns when fine particles (<125 μm) was removed, indicating small particle size was effective in removing bacteria.

Fine particles are known to increase the net surface area and contaminant removal by straining because of their occupancy of the spaces between sand and biochar grains

(Sasidharan et al., 2016). In our study, bacteria removal performance in columns with large biochar decreased faster than that observed in columns with smaller biochar sizes. The result indicates that fine fragments present in columns with large biochar was relatively larger than that present in columns with small biochar.

5. Conclusion

The results revealed the importance of biochar size on their performance in biofilters after compaction. The main conclusions are:

- After compaction, the total amount of particles released from biofilters is insignificant compared with the amount remained in the biofilters.
- Under compaction with similar energy as Standard Proctor method, biochar particles predominantly break by fragmentation irrespective of particle size, and the role of abrasion on the release of biochar particles after compaction is negligible.
- Hydraulic conductivity decreased and clogging potential increased after compaction, but the negative impact of compaction on hydraulic properties of biochar-augmented biofilters can be minimized by using large size biochar.
- Although the use of large size biochar may alleviate the impact of compaction on infiltration capacity of biofilters, contaminant removal capacity was lower when large biochar was used in the biofilters. The relatively high *E. coli* removal of biofilters augmented with small biochar compared with biofilters augmented with large biochar is attributed to the increase in surface area.

Particle breakage is governed by several factors such as particle size, shape, stress, impact velocity, particle micro-structure and particle strength. Results in this study demonstrated the breakage mechanism of biochar particles in a heterogeneous biofilter media, which could help to predict the possibility of biochar-bound contaminants to be released out of system based on the particle breakage mechanisms. This study provides changes in infiltration capacity and contaminant removal as well as biochar release potential and mechanism immediately after compaction. The compaction was simulated using Standard Proctor method so that the result can be compared with the other studies on compaction. However, the method does not

necessarily simulate the compaction conditions in field, which can be mild and may occur over a long period. Nevertheless, this is the first study that shows conceptually how biofilter-augmented with biochar may behave after compaction.

6. References

Ares, A., Terry, T. A., Miller, R. E., Anderson, H. W., & Flaming, B. L. (2005). Ground-based forest harvesting effects on soil physical properties and Douglas-fir growth. *Soil Science Society of America Journal. 69: 1822-1832*. Retrieved from

Berli, M., Kulli, B., Attinger, W., Keller, M., Leuenberger, J., Flühler, H., … Schulin, R. (2004). Compaction of agricultural and forest subsoils by tracked heavy construction machinery. *Soil and Tillage Research*, *75*(1), 37–52.

Boone, F. R. (1988). Weather and other environmental factors influencing crop responses to tillage and traffic. *Soil and Tillage Research*, *11*(3), 283–324.

Brusseau, M. L., Hu, Q., & Srivastava, R. (1997). Using flow interruption to identify factors causing nonideal contaminant transport. *Journal of Contaminant Hydrology*, *24*(3), 205–219.

Cambi, M., Certini, G., Neri, F., & Marchi, E. (2015). The impact of heavy traffic on forest soils: A review. *Forest Ecology and Management*, *338*, 124–138.

Chan, S. Y., Pilpel, N., & Cheng, D. C.-H. (1983). The tensile strengths of single powders and binary mixtures. *Powder Technology*, *34*(2), 173–189.

Currie, J. A. (1984). Gas diffusion through soil crumbs: The effects of compaction and wetting. *Journal of Soil Science*, *35*(1), 1–10.

Das, B. (2009). *Fundamentals of Geotechnical Engineering,* (Third). Chris Carson.

Das, O., Kim, N. K., Hedenqvist, M. S., Lin, R. J. T., Sarmah, A. K., & Bhattacharyya, D. (2018). An Attempt to Find a Suitable Biomass for Biochar-Based Polypropylene Biocomposites. *Environmental Management*, *62*(2), 403–413.

Frey, B., Kremer, J., Rüdt, A., Sciacca, S., Matthies, D., & Lüscher, P. (2009). Compaction of forest soils with heavy logging machinery affects soil bacterial community structure. *European Journal of Soil Biology*, *45*(4), 312–320.

Gold, M., Hogue, T., Pincetl, S., Mika, K., & Radavich, K. (2015). *Los Angeles Sustainable Water Project: Ballona Creek Watershed (Full Report)*.

Gupta, S. C., Sharma, P. P., & DeFranchi, S. A. (1989). Compaction Effects on Soil Structure11Contribution from the Department of Soil Science and the Minnesota Agricultural Experiment Station, University of Minnesota, St. Paul, MN 55108. Paper No. 15636, Science Journal Series. In N. C. Brady (Ed.), *Advances in Agronomy* (Vol. 42, pp. 311–338).

Hansen, S., & Ottino, J. M. (1997). Fragmentation with abrasion and cleavage: Analytical results. *Powder Technology*, *93*(2), 177–184.

Horn, R., Domżżał, H., Słowińska-Jurkiewicz, A., & van Ouwerkerk, C. (1995). Soil compaction processes and their effects on the structure of arable soils and the environment. *Soil and Tillage Research*, *35*(1), 23–36.

Liu, Z., Dugan, B., Masiello, C. A., Barnes, R. T., Gallagher, M. E., & Gonnermann, H. (2016). Impacts of biochar concentration and particle size on hydraulic conductivity and DOC leaching of biochar–sand mixtures. *Journal of Hydrology*, *533*, 461–472.
Mazzarotta, B. (1992). Abrasion and breakage phenomena in agitated crystal suspensions. *Chemical Engineering Science*, *47*(12), 3105–3111.

Mohanty, S., Cantrell, K., Nelson, K., & Boehm, A. (2014). Efficacy of biochar to remove Escherichia coli from stormwater under steady and intermittent flow. *Water Research*, *61*, 288–296.

Mohanty, S. K., & Boehm, A. B. (2014). Escherichia coli removal in biochar-augmented biofilter: Effect of infiltration rate, initial bacterial concentration, biochar particle size, and presence of compost. *Environmental Science & Technology*, *48*(19), 11535–11542.

Mohanty, S. K., Valenca, R., Berger, A. W., Yu, I. K. M., Xiong, X., Saunders, T. M., & Tsang, D. C. W. (2018). Plenty of room for carbon on the ground: Potential applications of biochar for stormwater treatment. *Science of The Total Environment*, *625*, 1644–1658.

Mossadeghi-Björklund, M., Arvidsson, J., Keller, T., Koestel, J., Lamandé, M., Larsbo, M., & Jarvis, N. (2016). Effects of subsoil compaction on hydraulic properties and preferential flow in a Swedish clay soil. *Soil and Tillage Research*, *156*, 91–98.

Neil, A. U., & Bridgwater, J. (1994). Attrition of particulate solids under shear. *Powder Technology*, *80*(3), 207–219.

Pitt, R., Chen, S., Clark, S., Swenson, J., & Ong, C. (2008). Compaction's Impacts on Urban StormWater Infiltration. *Journal of Irrigation and Drainage Engineering-Asce - J IRRIG DRAIN ENG-ASCE*, *134*.

Reynolds, G. K., Fu, J. S., Cheong, Y. S., Hounslow, M. J., & Salman, A. D. (2005). Breakage in granulation: A review. *Chemical Engineering Science*, *60*(14), 3969–3992.

Reza, M. T., Lynam, J., Vasquez, V. R., & Coronella, C. (2012). Pelletization of Biochar from Hydrothermally Carbonized Wood. *Environmental Progress*, *31*, 225–234.

Rodrigue, J.P., Comtois, C., Slack, B. (2017). *The Geography of Transport Systems: 4th Edition*. New York, NY: Routledge.

Sasidharan, S., Torkzaban, S., Bradford, S. A., Kookana, R., Page, D., & Cook, P. G. (2016). Transport and retention of bacteria and viruses in biochar-amended sand. *Science of The Total Environment*, *548–549*, 100–109.

Tavares, L. M., & King, R. P. (1998). Single-particle fracture under impact loading. *International Journal of Mineral Processing*, *54*(1), 1–28.

Walsh, C. J., Fletcher, T. D., & Burns, M. J. (2012). Urban Stormwater Runoff: A New Class of Environmental Flow Problem. *PLoS ONE*, *7*(9).

Wong, T., Breen, P., & Lloyd, S. (2000). *Water Sensitive Road Design – Design Options for Improving Stormwater Quality of Road Runoff*.

Yang, Y.-Y., & Toor, G. S. (2018). Stormwater runoff driven phosphorus transport in an urban residential catchment: Implications for protecting water quality in urban watersheds. *Scientific Reports*, *8*.

Zhang, X., & Baudet, B. A. (2013). Particle breakage in gap-graded soil. *Géotechnique Letters*, *3*(2), 72–77.